



HAL
open science

Climatic structures and intensities of the last two glacials documented by terrestrial molluscs from Chinese loess sequences

Dan Zhang, Nai-qin Wu, Feng-Jiang Li, Denis-Didier Rousseau, Xiao-Yun Chen, Ya-jie Dong, Hou-Yuan Lu

► **To cite this version:**

Dan Zhang, Nai-qin Wu, Feng-Jiang Li, Denis-Didier Rousseau, Xiao-Yun Chen, et al.. Climatic structures and intensities of the last two glacials documented by terrestrial molluscs from Chinese loess sequences. *Boreas*, 2021, 50 (1), pp.308-320. 10.1111/bor.12474 . hal-02992510

HAL Id: hal-02992510

<https://hal.science/hal-02992510>

Submitted on 10 Nov 2020

HAL is a multi-disciplinary open access archive for the deposit and dissemination of scientific research documents, whether they are published or not. The documents may come from teaching and research institutions in France or abroad, or from public or private research centers.

L'archive ouverte pluridisciplinaire **HAL**, est destinée au dépôt et à la diffusion de documents scientifiques de niveau recherche, publiés ou non, émanant des établissements d'enseignement et de recherche français ou étrangers, des laboratoires publics ou privés.

1
2
3
4 1 **Climatic structures and intensities of the last two glacials documented by**
5 2 **terrestrial mollusks from Chinese loess sequences**

6 3 DAN ZHANG, NAI-QIN WU, FENG-JIANG LI, DENIS-DIDIER ROUSSEAU, XIAO-YUN CHEN,
7 4
8 5 YA-JIE DONG AND HOU-YUAN LU
9 6

10 7 Zhang, D., Wu, N.-Q., Li F.-J., Rousseau, D.-D., Chen, X.-Y., Dong, Y.-J. & Lu, H.-Y.: Climatic
11 8 structures and intensities of the last two glacials documented by terrestrial mollusks from Chinese loess
12 9 sequences.
13 10

14 11 Knowledge of the structures and intensities of past glaciations is crucial for understanding Quaternary
15 12 palaeoclimatic evolution. Terrestrial mollusks are a reliable proxy of past environmental conditions and
16 13 can provide specific climatic insights into glacials. Here we compare the climatic evolution of the last
17 14 two glacials, based on mollusk fossils from the L2 and L1 loess units (equivalent to marine isotopic
18 15 stages (MIS) 6 and 4–2, respectively) of the Xifeng and Luochuan sections of the Chinese Loess
19 16 Plateau (CLP). The results show that both glacials had a tripartite structure but with different
20 17 intensities, as indicated by variations in the abundance of the dominant cold-aridiphilous mollusk
21 18 species, *Vallonia tenera* and *Pupilla aeoli*. The first stage, from ~191 to 184 ka for MIS 6, and from
22 19 ~71 to 57 ka for MIS 4, was characterized by a cold, arid climate, as indicated by the abundance of *V.*
23 20 *tenera* and *P. aeoli*, and the limited occurrence of thermo-humidiphilous (TH) species. The second
24 21 stage, from ~184 to 155 ka for MIS 6, and from ~57 to 29 ka for MIS 3, was characterized by a
25 22 relatively mild, humid climate, reflected by a decrease in *V. tenera* and *P. aeoli*, and an increase in TH
26 23 species. The last stage, from ~155 to 130 ka for MIS 6, and from ~29 to 11.7 ka for MIS 2, experienced
27 24 the coldest and driest conditions, as indicated by the dominance of *V. tenera* and *P. aeoli* in late MIS 6
28 25 and by the reduced occurrence of the grassland biomass, necessary for the growth of CA species, in
29 26 MIS 2. The climate during MIS 2 was much colder and drier than that during late MIS 6. We suggest
30 27 that the structures of the glacials were controlled mainly by insolation driven by changing astronomical
31 28 configurations, among which obliquity likely played the major role. The different glacial intensities
32 29 across the CLP may also have been related to variations in Northern Hemisphere ice sheets and the
33 30 temperature of the tropical oceans.
34 31

1
2
3 32 *Dan Zhang, Nai-Qin Wu (e-mail: nqwu@mail.iggcas.ac.cn), Feng-Jiang Li, Ya-Jie Dong and*
4 33 *Hou-Yuan Lu, Key Laboratory of Cenozoic Geology and Environment, Institute of Geology and*
5 34 *Geophysics, Chinese Academy of Sciences, Beijing 100029, China; Dan Zhang, Nai-Qin Wu and*
6 35 *Hou-Yuan Lu, College of Earth Sciences, University of Chinese Academy of Sciences, Beijing 100049,*
7 36 *China; Nai-Qin Wu and Feng-Jiang Li, Innovation Academy for Earth Science, Chinese Academy of*
8 37 *Sciences, Beijing 100029, China; Feng-Jiang Li, Center for Excellence in Life and Paleoenvironment,*
9 38 *Chinese Academy of Sciences, Beijing 100044, China; Denis-Didier Rousseau, Ecole Normale*
10 39 *Supérieure, Laboratoire de Météorologie Dynamique, UMR CNRS 8539, Paris 75231, France; Lamont*
11 40 *Doherty Earth Observatory of Columbia University, New York 10964, USA; Xiao-Yun Chen,*
12 41 *Geological Museum of China, Beijing 100034, China; Hou-Yuan Lu, Center for Excellence in Tibetan*
13 42 *Plateau Earth System Science, Chinese Academy of Sciences, Beijing 100101, China.*
14
15
16
17
18
19
20
21
22
23
24
25
26
27
28
29
30
31
32
33
34
35
36
37
38
39
40
41
42
43

For Review Only

1
2
3
4 44 The climate of the Quaternary period was characterized by the alternation of long, cold glacials and
5 45 short, warm interglacials (Hays *et al.* 1976; Shackleton *et al.* 1984; Lang & Wolff 2011).
6
7 46 Understanding the characteristics of different glacials is crucial for reconstructing the Quaternary
8
9 47 climatic history and for exploring the driving mechanisms of the glacial-interglacial cycles. In recent
10
11 48 years, numerous studies have focused on glacial climatic variations at orbital and millennial timescales
12
13 49 based on the study of marine, ice, and terrestrial (lake, loess, and speleothem) deposits (Hays *et al.*
14
15 50 1976; Dansgaard *et al.* 1993; Liu & Ding 1993; Porter & An 1995; Petit *et al.* 1999; Cheng *et al.*
16
17 51 2016). However, because most studies have focused on glacial inceptions and terminations, as well as
18
19 52 on abrupt climatic changes during glacials, the climatic structures and intensities of different glacials
20
21 53 remain poorly investigated.

22
23 54 The loess records from the Chinese Loess Plateau (CLP) of north-central China are of particular
24
25 55 value for investigating the structure and intensity of past glacials, and they have been used as evidence
26
27 56 in several important studies of the climatic variations of glacial cycles. Magnetic susceptibility (Kukla
28
29 57 & An 1989; An *et al.* 1991a) and chemical weathering indexes (Liu & Ding 1993; Guo *et al.* 1998)
30
31 58 have been widely used to document the effects of changing summer monsoon intensity, while the
32
33 59 grain-size record has been found to reflect the winter monsoon intensity (An *et al.* 1991b; Ding *et al.*
34
35 60 1995) and high-frequency climatic oscillations (Porter & An 1995; Ding *et al.* 1999). The carbon and
36
37 61 oxygen isotopic ratios in carbonate concretions from loess and palaeosol sequences have been used to
38
39 62 characterize variations in pedogenic intensity (Han *et al.* 1997; Liu & Ding 1993). Additionally,
40
41 63 mollusk assemblages have been regarded as reliable biological proxies that enable the interpretation of
42
43 64 past environmental conditions (Wu *et al.* 1996, 1997, 1999; Rousseau & Wu 1997, 1999).

44
45 65 Terrestrial mollusks are climatically sensitive and they are the only abundant biological remains
46
47 66 available for reconstructing the climatic variations preserved in European (Ložek 1964, 1990;
48
49 67 Rousseau 1985; Rousseau & Puisségur 1990), Chinese (Liu 1985; Wu *et al.* 1996, 1997, 1999, 2000)
50
51 68 and North American loess deposits (Rousseau & Kukla 1994; Rossignol *et al.* 2004). Terrestrial
52
53 69 mollusks are generally well-preserved in loess units, with shell dissolution occurring rarely – especially
54
55 70 in Chinese loess units – due to weak carbonate leaching and palaeosol development during glacials.
56
57 71 This is especially true for fossil records from the thick upper loess layers of the L2 and L1 units across
58
59 72 the CLP, which are the equivalents of marine isotopic stages (MIS) 6 and 4–2, respectively. These
60
73 73 thick loess layers can provide detailed palaeoenvironmental information which enables us to determine

1
2
3
4 74 the climatic structures and intensities of the corresponding glacials. In previous studies, Wu *et al.*
5 75 (1996, 1997, 1999, 2000) and Rousseau & Wu (1997, 1999) presented high-resolution records of
6 76 mollusk assemblages in Chinese loess sequences. Such records have been used to reconstruct
7 77 short-term climatic instability (Wu *et al.* 1999, 2002), long-term evolution of summer and winter
8 78 palaeo-monsoons (Wu *et al.* 1996, 2006, 2007; Li *et al.* 2006, 2008; Wu & Wu 2011), and their
9 79 potential relationships with orbital forcing (Wu *et al.* 2000, 2001; Li & Wu 2010). However,
10 80 distinctions in the climatic structures and intensities of different glacials themselves have not been
11 81 investigated in detail.

12
13
14
15
16
17
18
19 82 Here we present a new record of terrestrial mollusks from the L2 and L1 loess units of the Xifeng
20 83 section in the central CLP, which is combined with an equivalent record from the Luochuan section
21 84 (Wu *et al.* 1996, 1997, 1999, 2000; Rousseau & Wu 1997, 1999), with the aim of investigating the
22 85 climatic variability of the last two glacials.

23 86 24 87 Geographical background and site description

25 88 Loess-palaeosol sequences are extensively distributed in the CLP and alternations of the loess and
26 89 palaeosol layers in the CLP are well correlated with the marine oxygen isotope record, with loess layers
27 90 developed during glacials and palaeosols mainly during interglacials (Liu 1985; Kukla 1987). The
28 91 Xifeng (35°46'N, 107°41'E) and Luochuan (35°45'N, 109°25'E) sections, in the central CLP (Fig. 1),
29 92 are regarded as representative loess sequences for studying Quaternary climatic variations (e.g. Liu
30 93 1985; Kukla 1987; Kukla & An 1989; Wu *et al.* 1996, 1999; Rousseau & Wu 1997; Guo *et al.* 1998;
31 94 Hao *et al.* 2012). The modern climate of the CLP is influenced by the East Asian monsoon and is
32 95 characterized by in-phase variations in temperature and precipitation. The monsoon carries warm,
33 96 moist air to the CLP during the summer, which results in heavy rainfall. During the winter, monsoon
34 97 winds from the Siberian High prevail over the CLP, resulting in a dry, cold climate (Ding *et al.* 1995,
35 98 1999, 2002). The Xifeng section is ~160 km west of the Luochuan section.

36 99 The complete sequences of the Xifeng and Luochuan sections are ~176 m and ~137 m in
37 100 thickness, respectively (Liu 1985; Kukla & An 1989). The thicknesses of the L2 and L1 units are ~6 m
38 101 and ~10 m in Xifeng, and ~5 m and ~8.5 m in Luochuan (Fig. 2). These two units were deposited
39 102 during the last two glacials (Liu 1985; Kukla 1987) and correspond to MIS 6 (~191–130 ka) and MIS
40 103 4–2 (~71–11.7 ka) (Kukla 1987; Ding *et al.* 2002) (Fig. 2).

104 **Materials and methods**

105 A total of 164 mollusk fossil assemblages were analyzed at 10-cm intervals from the L2 and L1 loess
106 units of the Xifeng section (Table S1). Each sample weighed ~15 kg. Parallel to the mollusk samples,
107 we measured the low-field magnetic susceptibility every 10 cm using a portable Bartington magnetic
108 susceptibility meter. All mollusk samples were washed and sieved with a mesh diameter of 0.5 mm in
109 the field, and the mollusk shells were further sieved and dried in air. Subsequently, in the laboratory, all
110 mollusk fossils were picked out and identified under a binocular microscope. All identifiable remains
111 (whole shells and shell fragments) were considered in the total count of individuals following the
112 method of Puisségur (1976). The abundance of each species was expressed as the number of
113 individuals of that species per 15 kg of sediment. For the Luochuan section, 140 fossil snail
114 assemblages (Table S1) were analyzed using the same method, as described in Wu *et al.* (1996, 1999,
115 2000) and Rousseau & Wu (1997, 1999).

116 The uniformity of the stratigraphy of the loess deposits over hundreds of kilometers across the
117 CLP enabled us to apply a previously published chronology to our mollusk sequences (e.g. Liu 1985;
118 Kukla & An 1989; Ding *et al.* 2002; Hao *et al.* 2012). The chronology of the Xifeng and Luochuan
119 mollusk sequences was established using the correlations between our measured magnetic
120 susceptibility records and the recently published grain-size timescales of the Xifeng and Luochuan
121 sections (Hao *et al.* 2012) (Fig. 2, Table 1). Key age control points (Table 1) were defined by
122 comparing our magnetic susceptibility records with those of Hao *et al.* (2012).

123 *Vallonia tenera* and *Pupilla aeoli* are dominant cold-aridiphilous (CA) species in the fossil snail
124 assemblages in the CLP (Wu *et al.* 1996, 1999, 2000, 2001, 2002; Rousseau & Wu 1997, 1999). These
125 species prefer a relatively cold and arid environment, such as steppe and desert steppe (Wu *et al.* 2018).
126 In previous studies, the two species were commonly regarded as a proxy for the strength of the winter
127 monsoon (Wu *et al.* 1996, 1999, 2000, 2001, 2002, 2006; Li *et al.* 2006, 2008; Wu & Wu 2011), and
128 their abundance generally varies in parallel with global palaeoclimate curves reconstructed for the
129 associated marine isotopic stages (Fig. 2). Therefore, we used the abundances of the two species to
130 reconstruct past variations in the structure and intensity of glacials in the CLP.

131 Results

132 Fossil mollusk assemblages

133 Mollusks were abundant in the L2 and L1 loess units of the Xifeng and Luochuan sections; the average
134 shell concentrations were 220/15 kg and 206/15 kg, respectively. In the Xifeng section, 15 species were
135 identified from the L2 and L1 loess layers, and 23 species were identified in the Luochuan section.
136 Identifications were based on previously archived specimens and on the monographs of Yen (1939),
137 Chen & Gao (1987), and Nekola *et al.* (2015). The principal species are shown in Fig. 3. As in previous
138 studies (Liu 1985; Wu *et al.* 1996, 1999, 2000, 2001, 2002, 2007, 2018; Dong *et al.* 2019), the mollusk
139 species (Table 2) were subdivided into three ecological groups: cold-aridiphilous (CA),
140 cool-humidiphilous (CH), and thermo-humidiphilous (TH).

141 The CA group comprises *Vallonia tenera*, *Pupilla aeoli*, *Pupilla* cf. *muscorum*, *Cathaica*
142 *pulveraticula*, *Cathaica pulveratrix*, *Cathaica richthofen*, and *Cathaica* sp.. The CH group comprises a
143 single species, *Vallonia* cf. *pulchella*. The TH group comprises *Gastrocopta armigerella*, *Gastrocopta*
144 *coreana*, *Gastrocopta* sp., *Punctum orphana*, *Metodontia yantaiensis*, *Metodontia huaiensis*,
145 *Metodontia beresowskii*, *Metodontia* sp., *Succinea* sp., *Kaliella lamprocystis*, *Kaliella* sp.,
146 *Macrochlamys angigyra*, *Opeas striatissimum*, *Trichochloritis* sp., *Vitrea pygmaea*, *Vertigo*
147 *chenchiawoensis*, and Limacidae.

148 Xifeng section. – As shown in Fig. 4A, the composition of the mollusk assemblages from L2 (MIS 6)
149 exhibits a tripartite pattern, which is confirmed by the cluster analysis results. The CA species (e.g. *V.*
150 *tenera*, *P. aeoli* and *P.* cf. *muscorum* species) are dominant, whereas species from the CH and TH
151 groups are relatively rare. In the lower portion of L2 (~191–184 ka), the number of individuals of the
152 CA group increased rapidly to reach the maximum, from ~800 to ~1600/15 kg. Thereafter, during
153 ~184–155 ka, the number of individuals of the CA group decreased substantially to reach their lowest
154 concentration of ~80/15 kg. A few species of the CH and TH groups appeared simultaneously, such as
155 *V.* cf. *pulchella*, *G. armigerella*, *P. orphana*, and *Succinea* sp., mostly between ~184 and 160 ka.
156 Finally, in the upper part of L2 (~155–130 ka), the CA group increased again to reach a second
157 maximum, ~570/15kg; this interval is also characterized by the rarity of individuals of the TH group.

158 A tripartite division is also evident in L1 (Fig. 4A). In subunit L1-5 (~71–57 ka), the CA group
159 species (e.g. *V. tenera*, *P. aeoli* and *P.* cf. *muscorum*) were overwhelmingly dominant, and their

1
2
3
4 160 composition was similar to that of the lower part of L2. In subunits L1-4, L1-3, and L1-2 (~57–29 ka),
5
6 161 individuals of the CA group decreased while those of the CH and TH groups reappeared, similar to the
7
8 162 variations observed in the middle of L2. However, in subunit L1-1 (~29–11.7 ka), the composition of
9
10 163 the mollusk species differs substantially from that in the upper part of L2. Species of the CA and TH
11
12 164 groups in L1-1 were extremely rare. Furthermore, the total concentration of individuals (< 50/15 kg) in
13
14 165 L1-1 reached the lowest level overall, and in contrast to the upper part of L2, high concentrations of the
15
16 166 CA were not observed.

17
18 167 Luochuan section – The mollusk assemblages in the Luochuan section also reveal a tripartite structure
19
20 168 in L2 (Fig. 4B), which is similar to that of the Xifeng section. In the lower part of L2 (~191–184 ka),
21
22 169 the predominant species are *V. tenera* and *P. aeoli*, and the CA-group increased rapidly to a high
23
24 170 concentration (~800/15 kg) during this period. The abundance of the CA group decreased in the middle
25
26 171 part of L2 (~184–155 ka), with a minimum concentration of ~80/15 kg, whereas the abundances of the
27
28 172 TH and CH groups increased, from ~70 to ~280/15 kg. In the upper part of L2 (~155–130 ka), the
29
30 173 abundance of the CA group increased to another peak (~580/15 kg), accompanied by the decreasing
31
32 174 representation of the TH group.

33
34 175 The variations in the fossil mollusk species of L1 in the Luochuan section also exhibit a tripartite
35
36 176 structure (Fig. 4B). In subunit L1-5 (~71–57 ka), the composition of the snail assemblage shows a
37
38 177 similar pattern of variations to that of the lower part of L2, which is also dominated by species of the
39
40 178 CA group. The CA group also decreased in subunits L1-4, L1-3 and L1-2 (~57–29 ka), whereas the
41
42 179 species of the CH and TH groups both exhibit similar trends to those of the middle part of L2. A major
43
44 180 difference is evident between subunit L1-1 (~29–11.7 ka) and the upper part of L2: species of the CA
45
46 181 and TH groups were both extremely rare in subunit L1-1, whereas those of the CA group did not reach
47
48 182 higher values in the upper part of L2.

49
50 183 Units L2 and L1 of the Xifeng and Luochuan sections therefore show a similar trend of variation
51
52 184 of their fossil snail records over time. However, there were slight differences in species composition
53
54 185 between the two sections during the two glacials. First, the Xifeng section yielded a significant
55
56 186 proportion of the CA species *P. cf. muscorum* (Fig. 4A, B), whereas this species is poorly represented
57
58 187 in the Luochuan sequence. Second, the species compositions of the Xifeng and Luochuan sections are
59
60 188 different: the Xifeng section is characterized by *G. coreana* and *K. lamprocystis*, whereas the Luochuan
189 section is characterized by *C. pulveraticula*, *C. richthofen*, *Gastrocopta* sp., *M. beresowskii*, *O.*

1
2
3
4 190 *striatissimum*, *Kaliella* sp., *Trichochloritis* sp., *V. pygmaea*, *V. chenchiaowoensis*, and Limacidae. In
5
6 191 summary, despite minor variations in the mollusk assemblage composition, both sequences are
7
8 192 dominated by the CA group, and there is a low number of individuals of the TH group.

9
10 193 *Variations in V. tenera and P. aeoli during MIS 6 and MIS 4–2*

11 194 During the last two glacials, *V. tenera* and *P. aeoli* dominated the mollusk assemblages (>40–50%);
12
13 195 they have a similar ecological significance (Fig. 5). The variations in their total abundances are well
14
15 196 correlated with the marine isotope stages (Figs 2, 6), which reflects global glacial and interglacial
16
17 197 climatic oscillations. In some intervals, such as early MIS 6 (191–184 ka) and MIS 4 (71–57 ka), both
18
19 198 comprised more than ~80% of the total number of individuals. Furthermore, the numbers of individuals
20
21 199 of *V. tenera* and *P. aeoli* were also distributed continuously in units L2 and L1 units and they show the
22
23 200 same pattern of temporal variation in both sequences (Fig. 6). Therefore, we reconstructed the pattern
24
25 201 of climatic evolution of the last two glacials (i.e. their structure and intensity) based on the variations in
26
27 202 the abundances of these two species.

28
29 203 During the early part of MIS 6 (~191–184 ka), the maximum concentration of the sum of *V.*
30
31 204 *tenera* and *P. aeoli* in the Xifeng and Luochuan sections reached ~1200/15 kg (representing ~90% of
32
33 205 all species) and ~800/15 kg (representing ~95% of all species), respectively (Fig. 6). This interval is
34
35 206 also characterized by the presence of several TH members, such as the genus *Metodontia* (Fig. 4).
36
37 207 Subsequently, during ~184–155 ka, the concentrations of *V. tenera* and *P. aeoli* in both sections
38
39 208 decreased rapidly to a minimum of ~60/15 kg, representing ~70% of the individuals of all species in
40
41 209 the Xifeng section and ~30% in the Luochuan section. In addition, TH species were better represented,
42
43 210 including *G. armigerella*, *P. orphana*, Limacidae, and the genus *Metodontia* (Fig. 4). In the final stage
44
45 211 of MIS 6 (~155–130 ka), the total number of *V. tenera* and *P. aeoli* increased again and reached
46
47 212 ~520/15 kg in the Xifeng section (representing ~90% of all species), and ~560/15 kg in the Luochuan
48
49 213 section (representing ~95% of the individuals of all species). However, the CH and TH groups in late
50
51 214 MIS 6 were much less well-represented than in early MIS 6 (Fig. 4). Overall, the variations in *V. tenera*
52
53 215 and *P. aeoli* during MIS 6 show similar trends to the pattern of global changes indicated by the marine
54
55 216 isotope record (Fig. 6).

56
57 217 During MIS 4 (~71–57 ka), the maximum concentration of *V. tenera* and *P. aeoli* occurred in both
58
59 218 the Xifeng (~350/15 kg) and Luochuan sections (~460/15 kg) (Fig. 6), associated with a low number of
60
219 individuals of TH species (Fig. 4). During this period, both the CA and TH groups were represented by

220 a lower number of individuals than in early MIS 6 (Fig. 4). Subsequently, in MIS 3 (~57–29 ka), both
221 *V. tenera* and *P. aeoli* decreased at Xifeng (~20/15 kg) and Luochuan (~50/15 kg) representing ~50%
222 and ~30% of the number of individuals of all species, respectively (Fig. 6); however, there was a
223 significant increase in the counts of the TH species (Fig. 4), such as *G. armigerella*, *G. coreana*, *P.*
224 *orphana*, Limacidae, and the genus *Metodontia*.

225 Finally, during MIS 2 (~29–11.7 ka) (i.e. the Last Glacial Maximum, LGM), individuals of *V.*
226 *tenera* and *P. aeoli* were extremely rare in both the Xifeng and Luochuan sections (Fig. 6), and the total
227 number of the individuals of the CA and TH groups did not exceed 50/15 kg (Fig. 4). This interval is
228 also characterized by low values of magnetic susceptibility, reflecting cold and dry environmental
229 conditions (Fig. 4). The low number of mollusk individuals observed during this interval could not
230 have been caused by intensive decalcification, which occurs as a result of intensive pedogenic
231 processes associated with a warm and humid interglacial environment.

232 Discussion

233 As mentioned previously, the two studied loess sections, 160-km apart, yielded terrestrial mollusk
234 assemblages dominated by species of the CA group during the last two glacials. Although there are
235 slight differences in mollusk species composition in the two sections (Fig. 4), which may reflect local
236 conditions, our records clearly document changes in the structure and intensity of the last two glacials
237 on the orbital timescale.

238 Structure of the last two glacials in the CLP

239 The results (Figs 4, 6) show that the last two glacials (MIS 6 and MIS 4–2) had similar climatic
240 structures, consisting in both cases of two cold and dry intervals (the early and late stages) and a
241 relatively mild and humid intervening stage. This tripartite structure documented by our snail records
242 corresponds well to the global glacial structure revealed by sea level variations (Grant *et al.* 2014;
243 Spratt & Lisiecki 2016). Furthermore, these characteristics of glacials have also been documented
244 elsewhere, in terrestrial (Rousseau 1991; Tzedakis *et al.* 2006; Hao *et al.* 2012), marine (Bühring *et al.*
245 2004; Raymo *et al.* 2004), and ice (Petit *et al.* 1999) records. In terrestrial records, magnetic
246 susceptibility (Hao *et al.* 2012, 2015), organic carbon isotope composition ($\delta^{13}\text{C}_{\text{TOC}}$), and the
247 proportion of C4 plants (Zhou *et al.* 2016) from the CLP show higher values in the middle part of the
248 last two glacials compared with the early and late stages. Moreover, mollusk assemblages (Rousseau

1
2
3
4 249 1987, 1991) and tree pollen (Tzedakis *et al.* 2006) records from European loess sequences indicate that
5
6 250 both the TH mollusk species and arboreal pollen were more abundant during the middle part of the last
7
8 251 two glacials, whereas their abundances were very low during the early and late parts. This trend of
9
10 252 development is almost parallel to that of the mollusk records from the CLP. In marine and ice
11
12 253 sediments, such as the South China Sea (Bühring *et al.* 2004), North Atlantic (Raymo *et al.* 2004), and
13
14 254 Antarctic ice cores (Petit *et al.* 1999), the oxygen isotopic records exhibit prominent negative $\delta^{18}\text{O}$
15
16 255 excursions in the middle part of the last two glacials and positive values in the early and late parts.

17 256 *Intensity of the last two glacials in the CLP*

18
19 257 Our mollusk records show that the variations in glacial intensities within MIS 6 and MIS 4–2 were
20
21 258 different. During MIS 6, the most intense stage occurred in the later part, the second strongest stage
22
23 259 was in the early part, and a mild climatic stage occurred in the middle part. During the last glacial (MIS
24
25 260 4–2), the coldest and most arid climate occurred during MIS 2; in comparison, MIS 4 experienced less
26
27 261 cold and arid conditions, whereas relatively mild and humid interstadial conditions prevailed during
28
29 262 MIS 3.

30
31 263 The most prominent difference between the last two glacials is that the climatic conditions during
32
33 264 MIS 2 were much colder and more arid than those during the late stage of MIS 6. The extreme
34
35 265 environment of MIS 2 reduced the extent of the grassland environment necessary for the growth of the
36
37 266 CA species, resulting in a low total number of snail individuals (Fig. 4). A modern analog for the
38
39 267 conditions of MIS 2 has been found in Yakutia (Horsák *et al.* 2013). The much colder and drier
40
41 268 environment of MIS 2 in the CLP is also characterized by minima in organic carbon isotopes and of the
42
43 269 proportion of C4 plants (Zhou *et al.* 2016), and the dominance of desert steppe (Jiang *et al.* 2014). MIS
44
45 270 2 is also characterized by a higher ratio of herbs and *Pinus* to total pollen in a record from the South
46
47 271 China Sea (Sun *et al.* 2003), and by lower sea surface temperature (SST) in the South China Sea
48
49 272 (Herbert *et al.* 2010), Pacific Ocean (Liu & Herbert 2004), Indian Ocean (Herbert *et al.* 2010), and
50
51 273 Atlantic Ocean (Lawrence *et al.* 2009). Rousseau (1991) also inferred colder temperatures during MIS
52
53 274 2 from mollusk assemblages in European loess deposits. The results of a climate simulation indicated
54
55 275 that the atmospheric temperature of the Northern Hemisphere during MIS 2 was ~ 1.2 °C lower than
56
57 276 that during the late part of MIS 6 (Bintanja *et al.* 2005).

58 277 *Possible causes for structure and intensities of glacials in the CLP*

59
60 278 The similar structure of the last two glacials (MIS 6 and MIS 4–2) may have been caused primarily by

1
2
3
4 279 insolation variations driven by Earth orbital parameters, especially obliquity. The prominent increase in
5
6 280 the abundance of *V. tenera* and *P. aeoli* in both the early and late stages of glacials (Fig. 6) corresponds
7
8 281 approximately to periods of low obliquity (Fig. 7), and the decreases in their abundance in the middle
9
10 282 stages of glacials correspond to intervals of higher obliquity (Fig. 7). These observations agree with the
11
12 283 results of previous studies (Wu *et al.* 2000, 2001), which indicated that both the CA and TH mollusk
13
14 284 groups are tightly coupled to variation in obliquity, with a period of 41 kyr.

15 285 Obliquity is an important factor controlling the latitudinal distribution of insolation (Milankovitch
16
17 286 1941). During the early and late stages of the last two glacials, low obliquity reduced the summer
18
19 287 insolation at both northern high and middle latitudes and weakened the summer insolation gradient
20
21 288 between middle and low latitudes (Fig. 7). At high latitudes, the reduction of northern summer
22
23 289 insolation promoted ice sheet expansion, thereby enhancing the Asian winter monsoon which in turn
24
25 290 resulted in the passage of cold, dry air across the CLP (Ding *et al.* 1995); and at mid-latitudes, the
26
27 291 reduced insolation caused climatic cooling across the CLP. In addition, the decreasing insolation
28
29 292 gradient between northern low and middle latitudes (Fig. 7) limited the transport of heat and moisture
30
31 293 (Berger 1976; Young & Bradley 1984) from low-latitude oceans to the mid-latitude CLP, thus
32
33 294 weakening the strength of the summer monsoon circulation. Under the combined effects of these
34
35 295 factors, the glacial climatic conditions in the CLP became colder and more arid during the early and
36
37 296 late stages of the last two glacials, and the resulting environment favored the growth of members of the
38
39 297 CA group (Fig. 4), especially *V. tenera* and *P. aeoli*.

40 298 In contrast, during the middle intervals of the last two glacials, relatively high obliquity resulted in
41
42 299 increased summer insolation in northern high and middle latitudes, and in an increased summer
43
44 300 insolation gradient between northern middle and low latitudes (Laskar *et al.* 2004) (Fig. 7);
45
46 301 consequently, the strength of the winter monsoon was reduced. Conversely, the summer monsoon in
47
48 302 low to middle latitudes was enhanced, which increased the transport of heat and moisture from the
49
50 303 low-latitude oceans to the mid-latitude CLP. These combined effects weakened the glacial intensity
51
52 304 and resulted in relatively mild climatic conditions during the middle stages of the last two glacials,
53
54 305 which limited the growth of the mollusk species of the CA group, especially *V. tenera* and *P. aeoli*
55
56 306 (Fig. 6).

57
58 307 Although external astronomical factors, as discussed above, may have imparted the tripartite
59
60 308 structure of the last two glacials (MIS 6 and MIS 4–2), internal factors within the climate system may

1
2
3
4 309 also have influenced the variations in glacial intensity. The results of simulated ice sheet changes (Abe
5
6 310 *et al.* 2013) showed that the largest North American ice volume occurred in the late stages of the last
7
8 311 two glacials, corresponding to the increased abundance of *V. tenera* and *P. aeoli* in our records (Fig. 7),
9
10 312 both records indicating the occurrence of the coldest and most arid periods. The variations of European
11
12 313 ice sheet volume were only about half those of the North American ice sheets (Fig. 7) during the same
13
14 314 periods, which implies that North-American ice volume may have had a major role in the climate
15
16 315 system and therefore a greater impact on the CLP. The second largest North American ice sheet
17
18 316 volume occurred in the early stages of the last two glacials, in parallel with the variations of *V. tenera*
19
20 317 and *P. aeoli* (Fig. 7), both records documenting an intermediate glacial intensity. In the middle parts
21
22 318 of the glacials, a relatively low North American ice volume was associated with a lower abundance of
23
24 319 the individuals of *V. tenera* and *P. aeoli* (Fig. 7), and thus was closely related to relatively mild
25
26 320 climatic conditions in the CLP. Furthermore, the North American ice volume during MIS 2 was larger
27
28 321 than that during the late stage of MIS 6 (Bintanja *et al.* 2005; Abe *et al.* 2013) (Fig. 7), which was
29
30 322 related to a much greater glacial intensity during MIS 2 compared with MIS 6.

31 323 A second possible factor influencing the intensity of the last two glacials across the CLP may have
32
33 324 been tropical ocean circulation. Influenced by the Southeast Asian summer monsoon, the climate of the
34
35 325 CLP is sensitive to changes in the SST of the tropical Pacific and Indian oceans (Zhang & Lin 1985;
36
37 326 Liu & Ding 1993). Increased SST generally favors an increase in warm, humid airflows to the CLP.
38
39 327 Reconstructed SSTs for the tropical Pacific Ocean (Liu & Herbert 2004; Herbert *et al.* 2010) and
40
41 328 Indian Ocean (Herbert *et al.* 2010) indicate lowest SSTs during the late stages of the last two glacials,
42
43 329 less low SSTs during the early stages, and relative high SSTs during the middle stages. In addition,
44
45 330 marine records also indicate that the SST during MIS 2 was much lower than that during the late MIS 6
46
47 331 (Liu & Herbert 2004; Herbert *et al.* 2010). As a result, the heat transport capacity from the tropical
48
49 332 oceans to the CLP during MIS 2 was much weaker than during late MIS 6. Therefore, the much colder
50
51 333 tropical oceans and a larger Arctic ice sheet may have contributed to the extremely cold and arid
52
53 334 climatic conditions during MIS 2.

54 335 Overall, the combined influences of the variations in the Northern Hemisphere ice sheets and
55
56 336 changes in the circulation of the tropical oceans seemingly led to the observed diverse glacial
57
58 337 intensities in the CLP. The relatively large North American ice sheet and cooler tropical oceans may
59
60 338 have promoted a stronger glacial climate, while the smaller North American ice sheet and warm

339 tropical oceans resulted in a mild interstadial climate.

340

341 **Conclusions**

342 We have obtained terrestrial mollusk records from the L2 and L1 loess layers at two sites in the CLP,
343 and they indicate that the last two glacials both exhibit a tripartite structure but with different glacial
344 intensities. The first stage, from ~191 to 184 ka for MIS 6, and from ~71–57 ka for MIS 4, was
345 dominated by a cold, arid climate, as indicated by the abundance of *V. tenera* and *P. aeoli*, and the
346 limited occurrence of thermo-humidiphilous (TH) species. The second stage, from ~184 to 155 ka for
347 MIS 6, and from ~57 to 29 ka for MIS 3, was characterized by a relatively mild, humid climate, as
348 reflected by decreases in *V. tenera* and *P. aeoli*, and an increase in TH species. During the third stage,
349 from ~155 to 130 ka for MIS 6, and from ~29.0–11.7 ka for MIS 2, the climatic conditions of MIS 2
350 were much colder and drier than those during the late MIS 6 stage, which reduced the extent of
351 grassland environments necessary for the growth of both CA and TH species such that their
352 abundances were rare (< 50/15 kg).

353 We consider that the tripartite structure was mainly imparted by variations in obliquity. The cold,
354 arid climatic conditions during the early and late glacial stages may have been influenced by lower
355 obliquity that reduced the summer insolation at high latitudes and weakened the summer insolation
356 gradient between middle and low latitudes. The relatively mild, humid climate during the middle stage
357 of the glacials was primarily driven by a higher obliquity that reduced the Northern Hemisphere ice
358 volume and enhanced the transport of heat and moisture from low-latitude oceans to the mid-latitude
359 CLP. Hence, we suggest that glacial intensity was impacted by both external and internal factors.
360 Besides the external effects of obliquity, variations in Northern Hemisphere ice sheets and the
361 circulation of the tropical oceans may have played important roles in driving the observed variations in
362 glacial intensity at different times. Relatively small ice sheets and warm tropical oceans would have
363 promoted the mild, humid interstadial conditions during the middle stages of MIS 6 and MIS 3 in the
364 CLP. Relatively large ice sheets and cooler tropical oceans, on the other hand, may have strengthened
365 the cold, arid climate during the early and late stages of both glacials. Different from the cold, dry
366 climate during late MIS 6, MIS 2 was characterized by the coldest and most arid climate in the CLP
367 during the last two glacials, which may have been caused by a much larger North American ice sheet

1
2
3
4 368 and lower tropical SSTs. We note that further modelling simulations are needed to substantiate this
5
6 369 hypothesis.

7
8 370

9 371 *Acknowledgements.* – We thank Drs. Luo Wang, Qingzhen Hao, Xinxin Zuo, Xiaoyan Yang and Kai
10
11 372 Niu for constructive suggestions. Denis Didier Rousseau acknowledges Prof. Tungsheng Liu for
12
13 373 inviting him to collaborate with Chinese colleagues in the study of loess mollusks from the CLP. We
14
15 374 would like to thank Jan Bloemendal for English language editing. We are grateful to the two reviewers
16
17 375 for their useful suggestions and to Prof. Jan A. Piotrowski for his help in the correction of this paper.
18
19 376 This study was supported by the Strategic Priority Research Program of the Chinese Academy of
20
21 377 Sciences (grant No. XDB26000000) and the National Natural Science Foundation of China (grant Nos.
22
23 378 41430103, 41888101 and 41772186).

24
25 379 *Author contributions.* – NW, DZ, and HL conceived and designed the study. NW, FL, XC, DDR, and
26
27 380 YD undertook the field work. NW, XC, YD, and DDR collected and counted snail individuals. DZ, FL,
28
29 381 and DDR established the chronology of the studied sections. DZ, NW, FL, HL, DDR, XC, and YD
30
31 382 wrote the manuscript. DZ, NW, HL, FL, and DDR contributed to the interpretation of the results and
32
33 383 all the authors provided inputs to the final manuscript.

34
35 384

36 37 385 **References**

- 38
39 386 Abe, O. A., Saito, F., Kawamura, K., Raymo, M. E., Okuno, J. I., Takahashi, K. & Blatter, H. 2013:
40 387 Insolation-driven 100,000-year glacial cycles and hysteresis of ice-sheet volume. *Nature* 500,
41 388 190-194.
- 42
43 389 An, Z. S., Kukla, G., Porter, S. C. & Xiao, J. L. 1991a: Magnetic susceptibility evidence of monsoon
44 390 variation on the Loess Plateau of central China during the last 130,000 years. *Quaternary Research*
45 391 36, 29-36.
- 46
47 392 An, Z. S., Kukla, G., Porter, S. C. & Xiao, J. L. 1991b: Late Quaternary dust flow on the Chinese loess
48 393 plateau. *Catena* 18, 125-132.
- 49
50 394 Berger, A. 1976: Long-term variation of daily and monthly insolation during last Ice Age. *Eos*,
51 395 *Transactions American Geophysical Union* 57, 254-254.
- 52
53 396 Bintanja, R., Van, D. W., Roderik, S. W. & Oerlemans, J. 2005: Modelled atmospheric temperatures
54 397 and global sea levels over the past million years. *Nature* 437, 125-128.
- 55
56 398 Bühring, C., Sarnthein, M. & Erlenkeuser, H. 2004: Toward a high-resolution stable isotope
57 399 stratigraphy of the last 1.1 m.y.: Site 1144, South China Sea. In: Prell, W. L., Wang, P., Blum, P.,
58 400 Rea, D. K., Clemens, S. C. (eds.): *Proceedings of the Ocean Drilling Program. Scientific Results*
59 401 184, 1-29.
- 60 402 Chen, D. N. & Gao, J. X. 1987: *Economic Fauna Sinica of China, Terrestrial Mollusca*. 186 pp.

1
2
3
4
5
6
7
8
9
10
11
12
13
14
15
16
17
18
19
20
21
22
23
24
25
26
27
28
29
30
31
32
33
34
35
36
37
38
39
40
41
42
43
44
45
46
47
48
49
50
51
52
53
54
55
56
57
58
59
60

- 403 Science Press, Beijing (in Chinese).
- 404 Cheng, H., Edwards, R. L., Sinha, A., Spötl, C., Yi, L., Chen, S. T., Kelly, M., Kathayat, G., Wang, X.
405 F., Li, X. L., Kong, X. G., Wang, Y. J., Ning, Y. F. & Zhang, H. W. 2016: The Asian monsoon
406 over the past 640,000 years and ice age terminations. *Nature* 534, 640-646.
- 407 Dansgaard, W., Johnsen, S. J., Clausen, H. B., Dahljensen, D., Gundestrup, N. S., Hammer, C. U.,
408 Hvidberg, C. S., Steffensen, J. P., Sveinbjornsdottir, A. E., Jouzel, J. & Bond, G. 1993: Evidence
409 for General Instability of Past Climate from a 250-Kyr Ice-Core Record. *Nature* 364, 218-220.
- 410 Ding, Z. L., Liu, T. S., Rutter, N. W., Yu, Z. W., Guo, Z. T. & Zhu, R. X. 1995: Ice-volume forcing of
411 East Asian winter monsoon variations in the past 800,000 years. *Quaternary Research* 44,
412 149-159.
- 413 Ding, Z. L., Ren, J. Z., Yang, S. L. & Liu, T. S. 1999: Climate instability during the penultimate
414 glaciation: Evidence from two high-resolution loess records, China. *Journal of Geophysical*
415 *Research: Solid Earth* 104, 20123-20132.
- 416 Ding, Z. L., Derbyshire, E., Yang, S. L., Yu, Z. W., Xiong, S. F. & Liu, T. S. 2002: Stacked 2.6-Ma
417 grain size record from the Chinese loess based on five sections and correlation with the deep-sea
418 $\delta^{18}\text{O}$ record. *Paleoceanography* 17, doi 10.1029/2001PA000725.
- 419 Dong, Y. J., Wu, N. Q., Li, F. J., Chen, X. Y., Zhang, D., Zhang, Y. T., Huang, L. P., Wu, B. & Lu, H.
420 Y. 2019: Influence of monsoonal water-energy dynamics on terrestrial mollusk species-diversity
421 gradients in northern China. *Science of The Total Environment* 676, 206-214.
- 422 Grant, K. M., Rohling, E. J., Ramsey, C. B., Cheng, H., Edwards, R. L., Florindo, F., Heslop, D.,
423 Marra, F., Roberts, A. P., Tamisiea, M. E. & Williams, F. 2014: Sea-level variability over five
424 glacial cycles. *Nature Communications* 5, doi 10.1038/ncomms6076.
- 425 Guo, Z. T., Liu, T. S., Fedoroff, N., Wei, L. Y., Ding, Z. L., Wu, N. Q., Lu, H. Y., Jiang, W. Y. & An,
426 Z. S. 1998: Climate extremes in loess of China coupled with the strength of deep-water formation
427 in the North Atlantic. *Global and Planetary Change* 18, 113-128.
- 428 Hao, Q. Z., Wang, L., Oldfield, F., Peng, S. Z., Qin, L., Song, Y., Xu, B., Qiao, Y. S., Bloemendal, J.
429 & Guo, Z. T. 2012: Delayed build-up of Arctic ice sheets during 400,000-year minima in
430 insolation variability. *Nature* 490, 393-396.
- 431 Hao, Q. Z., Wang, L., Oldfield, F. & Guo, Z. T. 2015: Extra-long interglacial in Northern Hemisphere
432 during MISs 15-13 arising from limited extent of Arctic ice sheets in glacial MIS 14. *Scientific*
433 *reports* 5, doi 10.1038/srep12103.
- 434 Han, J. M., Keppens, E., Liu, T. S., Paepe, R. & Jiang, W. Y. 1997: Stable isotope composition of the
435 carbonate concretion in loess and climate change. *Quaternary International* 37, 37-43.
- 436 Hays, J. D., Imbrie, J. & Shackleton, N. J. 1976: Variations in earths orbit-pacemaker of ice ages.
437 *Science* 194, 1121-1132.
- 438 Herbert, T. D., Peterson, L. C., Lawrence, K. T. & Liu, Z. H. 2010: Tropical ocean temperatures over
439 the past 3.5 million years. *Science* 328, 1530-1534.
- 440 Horsák, M., Chytrý, M. & Axmanová, I. 2013: Exceptionally poor land snail fauna of central Yakutia
441 (NE Russia): climatic and habitat determinants of species richness. *Polar Biology* 36, 185-191.
- 442 Jiang, W. Y., Yang, X. X. & Cheng, Y. F. 2014: Spatial patterns of vegetation and climate on the
443 Chinese Loess Plateau since the Last Glacial Maximum. *Quaternary international* 334, 52-60.
- 444 Kukla, G. 1987: Loess stratigraphy in central China. *Quaternary Science Reviews* 6, 191-219.
- 445 Kukla, G. & An, Z. 1989: Loess stratigraphy in central China. *Palaeogeography, Palaeoclimatology,*
446 *Palaeoecology* 72, 203-225.

- 1
2
3 447 Lang, N. & Wolff, E. W. 2011: Interglacial and glacial variability from the last 800 ka in marine, ice
4 448 and terrestrial archives. *Climate of the Past* 7, 361-380.
- 5 449 Laskar, J., Robutel, P., Joutel, F., Gastineau, M., Correia, A. C. M. & Levrard, B. 2004: A long-term
6 450 numerical solution for the insolation quantities of the Earth. *Astronomy & Astrophysics* 428,
7 451 261-285.
- 8 452 Lawrence, K. T., Herbert, T. D., Brown, C. M., Raymo, M. E. & Haywood, A. M. 2009:
9 453 High-amplitude variations in North Atlantic sea surface temperature during the early Pliocene
10 454 warm period. *Paleoceanography* 24, doi 10.1029/2008PA001669.
- 11 455 Li, F. J., Wu, N. Q., Pei, Y. P., Hao, Q. Z. & Rousseau, D. D. 2006: Wind-blown origin of Dongwan
12 456 late Miocene–Pliocene dust sequence documented by land snail record in western Chinese Loess
13 457 Plateau. *Geology* 34, 405-408.
- 14 458 Li, F. J., Rousseau, D. D., Wu, N. Q., Hao, Q. Z. & Pei, Y. P. 2008: Late Neogene evolution of the East
15 459 Asian monsoon revealed by terrestrial mollusk record in Western Chinese Loess Plateau: from
16 460 winter to summer dominated sub-regime. *Earth and Planetary Science Letters* 274, 439-447.
- 17 461 Li, F. J. & Wu, N. Q. 2010: Pliocene land snail record from western Chinese Loess Plateau and
18 462 implications for impacts of the summer insolation gradient between middle and low latitudes on
19 463 the East Asian summer monsoon. *Global and Planetary Change* 72, 73-78.
- 20 464 Lisiecki, L. E. & Raymo, M. E. 2005: A Pliocene-Pleistocene stack of 57 globally distributed benthic
21 465 $\delta^{18}\text{O}$ records. *Paleoceanography* 20, doi 10.1029/2004PA001071.
- 22 466 Liu, T. S. 1985: *Loess and the Environment*. 251 pp. China Ocean Press, Beijing (in Chinese).
- 23 467 Liu, T. S. & Ding, Z. L. 1993: Stepwise coupling of monsoon circulations to global ice volume
24 468 variations during the late Cenozoic. *Global and Planetary Change* 7, 119-130.
- 25 469 Liu, Z. H. & Herbert, T. D. 2004: High-latitude influence on the eastern equatorial Pacific climate in
26 470 the early Pleistocene epoch. *Nature* 427, 720-723.
- 27 471 Ložek, V. 1964: Quartärmollusken der Tschechoslowakei. *Rozpravy Ústředního ústavu geologického*
28 472 31, 1-374.
- 29 473 Ložek, V. 1990: Molluscs in loess, their paleoecological significance and role in
30 474 geochronology—Principles and methods. *Quaternary International* 77, 1-79.
- 31 475 Milankovitch, M. 1941: *Kanon der Erdebstrahlung und seine Anwendung auf das Eiszeitenproblem*.
32 476 484 pp. Stamparija Mihaila Ćurčića, Beograd. (Translated version, 1998: *Canon of Insolation and*
33 477 *the Ice-age Problem*. Zavod za udžbenike i nastavna sredstva)
- 34 478 Nekola, J. C., Coles, B. F. & Horsak, M. 2015: Species assignment in *Pupilla* (Gastropoda: Pulmonata:
35 479 Pupillidae): integration of DNA-sequence data and conchology. *Journal of Molluscan Studies* 81,
36 480 196-216.
- 37 481 Petit, J. R., Jouzel, J., Raynaud, D., Barkov, N. I., Barnola, J. M., Basile, I., Bender, M., Chappellaz, J.,
38 482 Davis, M., Delaygue, G., Delmotte, M., Kotlyakov, V. M., Legrand, M., Lipenkov, V. Y., Lorius,
39 483 C., Pepin, L., Ritz, C., Saltzman, E. & Stievenard, M. 1999: Climate and atmospheric history of
40 484 the past 420,000 years from the Vostok ice core, Antarctica. *Nature* 399, 429-436.
- 41 485 Porter, S. C. & An, Z. S. 1995: Correlation between climate events in the North Atlantic and China
42 486 during the last glaciation. *Nature* 375, 305-308.
- 43 487 Puisségur, J. J. 1976: *Mollusques continentaux quaternaires de Bourgogne: significations*
44 488 *stratigraphiques et climatiques. Rapports avec d'autres faunes boréales de France*. 241pp. Centre de
45 489 *Paléogéographie et de Paléobiologie Evolutives, Université de Dijon*.
- 46 490 Raymo, M. E., Oppo, D. W., Flower, B. P., Hodell, D. A., Mcmanus, J. F., Venz, K. A., Kleiven, K. F.

1
2
3
4
5
6
7
8
9
10
11
12
13
14
15
16
17
18
19
20
21
22
23
24
25
26
27
28
29
30
31
32
33
34
35
36
37
38
39
40
41
42
43
44
45
46
47
48
49
50
51
52
53
54
55
56
57
58
59
60

- 491 & McIntyre, K. 2004: Stability of North Atlantic water masses in face of pronounced climate
492 variability during the Pleistocene. *Paleoceanography* 19, doi 10.1029/2003PA000921.
- 493 Rossignol, J., Moine, O. & Rousseau, D. D. 2004: The Buzzard's Roost and Eustis mollusc sequences:
494 comparison between the paleoenvironments of two sites in the Wisconsinan loess of Nebraska,
495 USA. *Boreas* 33, 145-154.
- 496 Rousseau, D. D. 1985: Structures des populations quaternaires de pupilla muscorum (gastropode) en
497 Europe du Nord: relations avec leurs environnements. *Geobios* 18, 407.
- 498 Rousseau, D. D. 1987: Paleoclimatology of the Achenheim series (middle and upper pleistocene,
499 Alsace, France). A malacological analysis. *Palaeogeography, Palaeoclimatology, Palaeoecology*
500 59, 293-314.
- 501 Rousseau, D. D. & Puisségur, J. J. 1990: A 350,000-year climatic record from the loess sequence of
502 Achenheim, Alsace, France. *Boreas* 19, 203-216.
- 503 Rousseau, D. D. 1991: Climatic transfer function from Quaternary molluscs in European loess deposits.
504 *Quaternary Research* 36, 195-209.
- 505 Rousseau, D. D. & Kukla, G. 1994: Late Pleistocene climate record in the Eustis loess section,
506 Nebraska, based on land snail assemblages and magnetic susceptibility. *Quaternary Research* 42,
507 176-187.
- 508 Rousseau, D. D. & Wu, N. Q. 1997: A new molluscan record of the monsoon variability over the past
509 130 000 yr in the Luochuan loess sequence, China. *Geology* 25, 275-278.
- 510 Rousseau, D. D. & Wu, N. Q. 1999: Mollusk record of monsoon variability during the L2-S2 cycle in
511 the Luochuan loess sequence, China. *Quaternary Research* 52, 286-292.
- 512 Shackleton, N. J., Backman, J., Zimmerman, H. T., Kent, D. V., Hall, M. A., Roberts, D. G., Schnitker,
513 D., Baldauf, J. G., Desprairies, A. & Homrighausen, R. 1984: Oxygen isotope calibration of the
514 onset of ice-rafting and history of glaciation in the North Atlantic region. *Nature* 307, 620-623.
- 515 Spratt, R. M. & Lisiecki, L. E. 2016: A Late Pleistocene sea level stack. *Climate of the Past*
516 Discussions 11, 3699-3728.
- 517 Sun, X. J., Luo, Y. L., Huang, F., Tian, J. & Wang, P. X. 2003: Deep-sea pollen from the South China
518 Sea: Pleistocene indicators of East Asian monsoon. *Marine Geology* 201, 97-118.
- 519 Tzedakis, P. C., Hooghiemstra, H. & Pälike, H. 2006: The last 1.35 million years at Tenaghi Philippon:
520 revised chronostratigraphy and long-term vegetation trends. *Quaternary Science Reviews* 25,
521 3416-3430.
- 522 Wu, B. & Wu, N. Q. 2011: Terrestrial mollusc records from Xifeng and Luochuan L9 loess strata and
523 their implications for paleoclimatic evolution in the Chinese Loess Plateau during marine Oxygen
524 Isotope Stages 24-22. *Climate of the Past* 7, 349-359.
- 525 Wu, N. Q., Rousseau, D. D. & Liu, D. S. 1996: Land mollusk records from the Luochuan loess
526 sequence and their paleoenvironmental significance. *Science in China: Series D Earth Sciences*
527 39, 494-502.
- 528 Wu, N. Q., Lu, H. Y. & Guo, Z. T. 1997: Reconstruction of paleoclimate in the Loess Plateau using
529 non-linear mathematical methods. *Chinese Science Bulletin* 42: 1014-1016.
- 530 Wu, N. Q., Rousseau, D. D. & Liu, D. S. 1999: Climatic instability recorded by the mollusk
531 assemblages from the late glacial loess deposits in China. *Chinese science bulletin* 44, 1238-1242.
- 532 Wu, N. Q., Rousseau, D. D. & Liu, X. P. 2000: Response of mollusk assemblages from the Luochuan
533 loess section to orbital forcing since the last 250 ka. *Chinese Science Bulletin* 45, 1617-1622.
- 534 Wu, N. Q., Rousseau, D. D., Liu, T. S., Lu, H. Y., Gu, Z. Y., Guo, Z. T. & Jiang, W. Y. 2001: Orbital

- 1
2
3 535 forcing of terrestrial mollusks and climatic changes from the Loess Plateau of China during the
4 536 past 350 ka. *Journal of Geophysical Research: Atmospheres* 106, 20045-20054.
- 5 537 Wu, N. Q., Liu, T. S., Liu, X. P. & Gu, Z. Y. 2002: Mollusk record of millennial climate variability in
6 538 the Loess Plateau during the Last Glacial Maximum. *Boreas* 31, 20-27.
- 7 539 Wu, N. Q., Pei, Y. P., Lu, H. Y., Guo, Z. T., Li, F. J. & Liu, T. S. 2006: Marked ecological shifts
8 540 during 6.2–2.4 Ma revealed by a terrestrial molluscan record from the Chinese Red Clay
9 541 Formation and implication for palaeoclimatic evolution. *Palaeogeography, Palaeoclimatology,*
10 542 *Palaeoecology* 233, 287-299.
- 11 543 Wu, N. Q., Chen, X. Y., Rousseau, D. D., Li, F. J., Pei, Y. P. & Wu, B. 2007: Climatic conditions
12 544 recorded by terrestrial mollusc assemblages in the Chinese Loess Plateau during marine Oxygen
13 545 Isotope Stages 12–10. *Quaternary Science Reviews* 26, 1884-1896.
- 14 546 Wu, N. Q., Li, F. J. & Rousseau, D. D. 2018: Terrestrial mollusk records from Chinese loess sequences
15 547 and changes in the East Asian monsoonal environment. *Journal of Asian Earth Sciences* 155,
16 548 35-48.
- 17 549 Yen, T. C. 1939: Die Chinesischen Land- und Süßwasser-Gastropoden des Natur-Museums
18 550 Senckenberg. *Abhandlungen der Senckenbergischen Naturforschenden Gesellschaft* 444, 1–235.
- 19 551 Young, M. A. & Bradley, R. S. 1984: Insolation gradients and the paleoclimatic record. In: Berger
20 552 Imbrie, J., Hays, J., Kukla, G. & Saltzman B. (eds.): *Milankovitch and Climate*. NATO ASI Series
21 553 (Series C: Mathematical and Physical Sciences) 126, 707–713. Springer, Dordrecht.
- 22 554 Zhang, J. C. & Lin, Z. G. 1985: *Climate of China*. 607 pp. Shanghai Scientific and Technical
23 555 Publishers, Shanghai (in Chinese).
- 24 556 Zhou, B., Wali, G., Peterse, F. & Bird, M. I. 2016: Organic carbon isotope and molecular fossil records
25 557 of vegetation evolution in central Loess Plateau since 450 kyr. *Science China Earth Sciences* 59,
26 558 1206-1215.
- 27 559
- 28
29
30
31
32
33
34
35
36
37
38
39
40
41
42
43
44
45
46
47
48
49
50
51
52
53
54
55
56
57
58
59
60

1
2
3
4
5
6
7
8
9
10
11
12
13
14
15
16
17
18
19
20
21
22
23
24
25
26
27
28
29
30
31
32
33
34
35
36
37
38
39
40
41
42
43
44
45
46
47
48
49
50
51
52
53
54
55
56
57
58
59
60

560 Figure 1. Location of the study sites in the CLP. A. Inset map shows the location of the CLP and the
561 pathways of the East Asian winter monsoon (EAWM) (blue arrows) and summer monsoon (EASM)
562 (red arrows); B. Map of the CLP showing the locations of the Xifeng and Luochuan sections (blue
563 triangles).

564 Figure 2. Comparison of the variations in magnetic susceptibility (MS, grey lines) and the abundance
565 of *Vallonia tenera* and *Pupilla aeoli* (VP, purple lines) from the Xifeng and Luochuan sections (this
566 study), a previously published magnetic susceptibility record (red lines) (Hao *et al.* 2012), and the
567 LR04 marine oxygen isotope stack (blue line). S = palaeosol; L = loess; LR04 is benthic $\delta^{18}\text{O}$ stack of
568 57 global records compiled by Lisiecki & Raymo (2005). 1-7 = Marine Isotope Stages 1-7.

569 Figure 3. Typical mollusk species identified in the L2 and L1 units of the Xifeng and Luochuan
570 sections. 1 and 2 = *Pupilla aeoli*; 3 and 4 = *Pupilla cf. muscorum*; 5-7 = *Vallonia tenera*; 8-10 =
571 *Punctum orphana*; 11-13 = *Cathaica pulveratrix*; 14-16 = *Cathaica* sp. The scale bars represent 1 mm.

572 Figure 4. Variations in the counts of whole mollusks in the upper two loess units (L2 and L1) of the
573 Xifeng section (A), and the Luochuan section (B) (number of individuals counted per 15 kg).
574 Cold-aridiphilous (CA, dark blue solid shading), cool-humidiphilous (CH, light blue shading),
575 thermo-humidiphilous (TH, red shading) species; total mollusk individuals (black shading), sum of the
576 number of mollusk species (blue line), and the results of a cluster analysis of the assemblages. The light
577 blue background represents cold, dry glacial periods, and the light orange background represents mild,
578 humid interstadial periods. S = palaeosol; L = loess; MS = magnetic susceptibility; CONISS =
579 constrained incremental sum of squares; MIS = Marine Isotopic Stage.

580 Figure 5. Results of hierarchical cluster analysis of all of the mollusk species within the interval of
581 L2-S0 (L = loess; S = palaeosol) at Xifeng (A) and Luochuan (B). The Y axis represents the distance
582 between the identified species and the cluster center.

583 Figure 6. Variations in the total of *V. tenera* and *P. aeoli* (VP) in the upper two loess units (L2 and L1)
584 of the Xifeng and Luochuan sections. Magnetic susceptibility (MS, orange lines), VP individuals
585 (purple lines, on a reversed scale), VP percentages (black lines, on a reversed scale), and the LR04
586 marine $\delta^{18}\text{O}$ stack (blue line, on a reversed scale). The Luochuan data are from Wu *et al.* (1996, 1999,
587 2000) and Rousseau & Wu (1997, 1999). The light blue background represents cold, dry glacial
588 periods, and the light orange background represents mild, humid interstadial periods. The red stippled
589 area indicates period in which snail fossils were rare (<50/15 kg). LR04 is a benthic $\delta^{18}\text{O}$ stack of 57
590 global records compiled by Lisiecki & Raymo (2005). MIS = Marine Isotopic Stage.

591 Figure 7. Comparison of profiles of the counts of *V. tenera* and *P. aeoli* (VP, purple lines) in loess units
592 L2 and L1 of the Xifeng and Luochuan sequences with records of North American and European ice
593 volume (equivalent to sea level) (Bintanja *et al.* 2005), the LR04 benthic $\delta^{18}\text{O}$ stack (Lisiecki & Raymo
594 2005), and Earth orbital parameters (obliquity, precession, 65°N insolation and the mean summer
595 insolation gradient between 35°N and 0°) (Laskar *et al.* 2004). The light blue background represents
596 cold, dry glacial periods, and the light orange background represents mild, humid interstadial periods.

1
2
3
4 597 The red stippled areas are intervals in which snail fossils were rare (< 50/15 kg). LR04 is a benthic
5 598 $\delta^{18}\text{O}$ stack comprising 57 global records compiled by Lisiecki & Raymo (2005). MIS = Marine
6 599 Isotopic Stage. Note that several X axes are reversed so that the warming occurs in a consistent
7 600 direction (i.e. to the right).
8
9

10 601 Table 1. Selected age-control points for the Xifeng and Luochuan profiles, used to establish a
11 602 chronology via comparison with a grain-size age model of Hao *et al.* (2012).
12
13

14 603 Table 2. List of mollusk species identified in loess units L2 and L1 of the Xifeng and Luochuan
15 604 sections
16
17

18 605
19
20
21
22
23
24
25
26
27
28
29
30
31
32
33
34
35
36
37
38
39
40
41
42
43
44
45
46
47
48
49
50
51
52
53
54
55
56
57
58
59
60

For Review Only

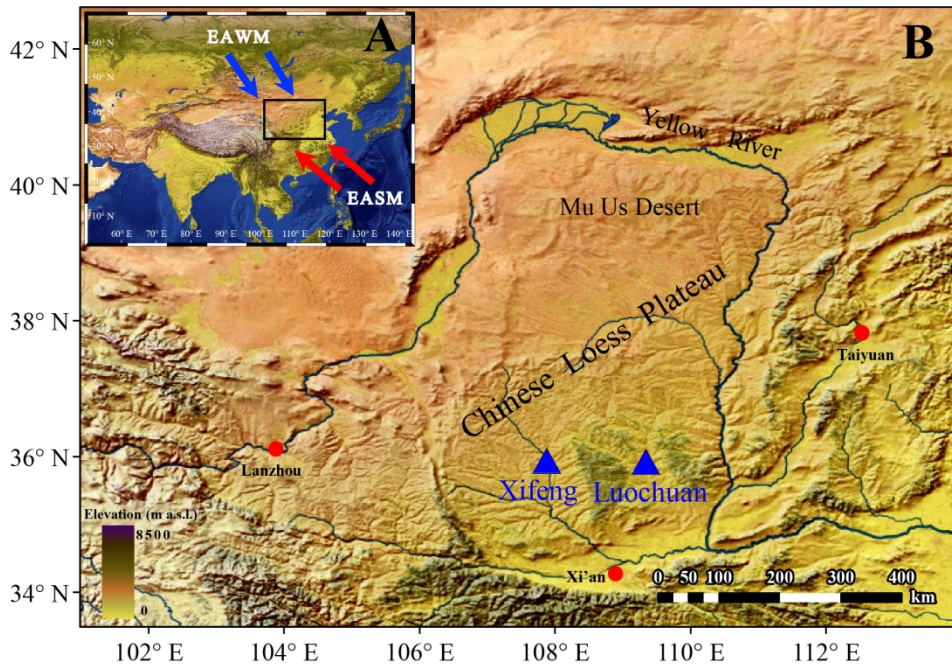
1
2
3
4
5
6
7
8
9
10
11
12
13
14
15
16
17
18
19
20
21
22
23
24
25
26
27
28
29
30
31
32
33
34
35
36
37
38
39
40
41
42
43
44
45
46
47
48
49
50
51
52
53
54
55
56
57
58
59
60

606 Supporting information

607 Table S1. Dataset of the number of *Vallonia tenera* and *Pupilla aeoli* (VP) individuals in loess units L2
608 and L1 of the Xifeng section.

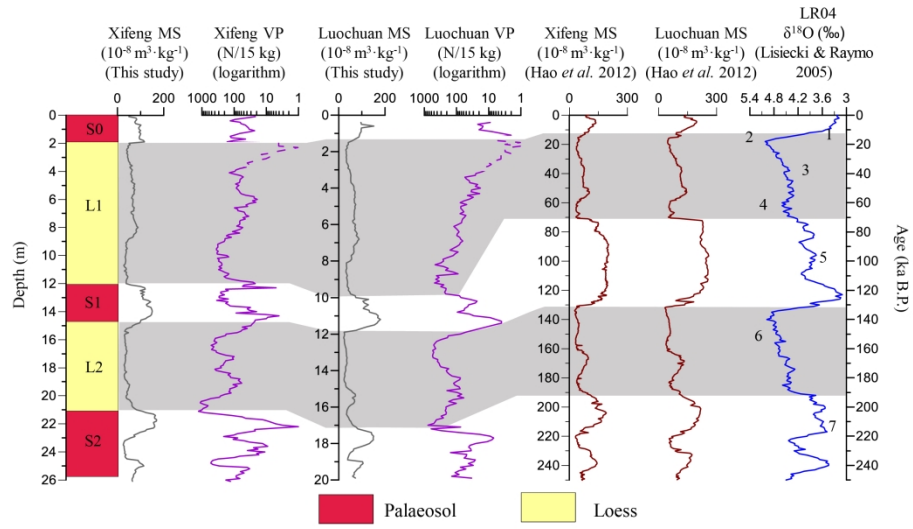
609 Table S2. Dataset of the number of *Vallonia tenera* and *Pupilla aeoli* (VP) individuals in loess units L2
610 and L1 from the Luochuan section.

For Review Only

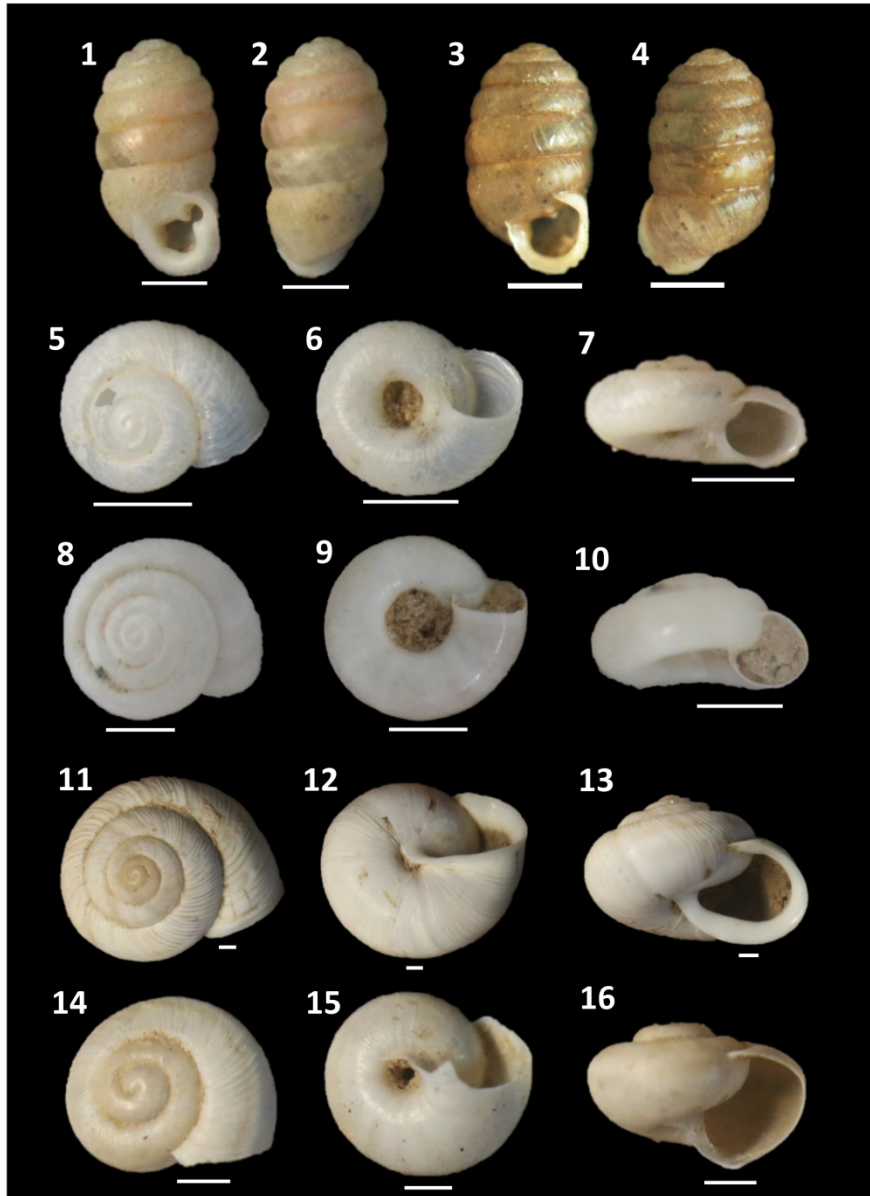


196x136mm (300 x 300 DPI)

1
2
3
4
5
6
7
8
9
10
11
12
13
14
15
16
17
18
19
20
21
22
23
24
25
26
27
28
29
30
31
32
33
34
35
36
37
38
39
40
41
42
43
44
45
46
47
48
49
50
51
52
53
54
55
56
57
58
59
60

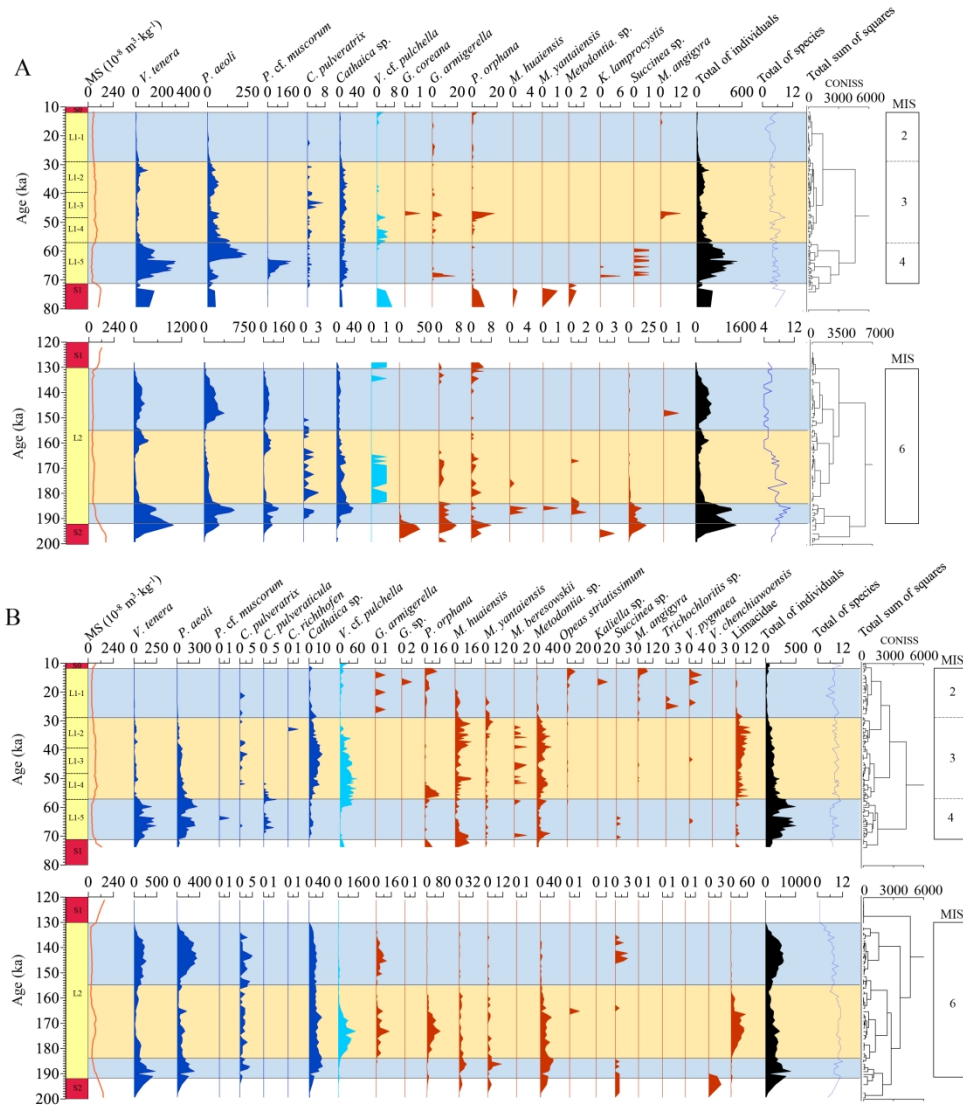


260x160mm (300 x 300 DPI)

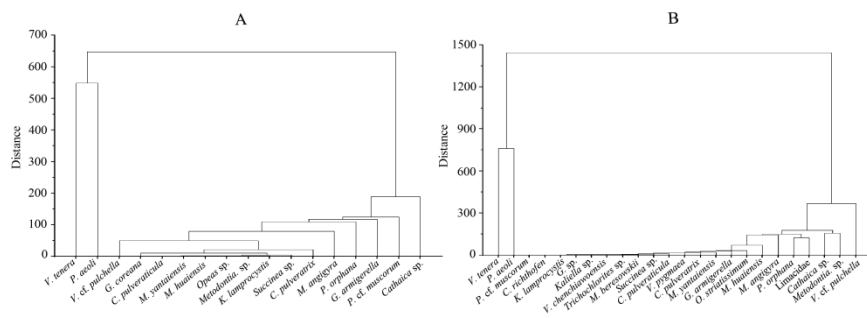


176x235mm (300 x 300 DPI)

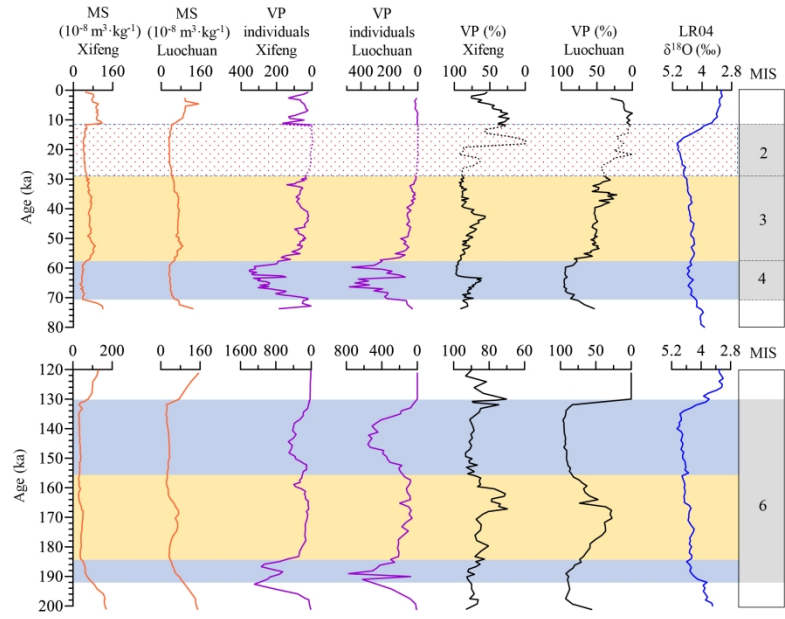
1
2
3
4
5
6
7
8
9
10
11
12
13
14
15
16
17
18
19
20
21
22
23
24
25
26
27
28
29
30
31
32
33
34
35
36
37
38
39
40
41
42
43
44
45
46
47
48
49
50
51
52
53
54
55
56
57
58
59
60



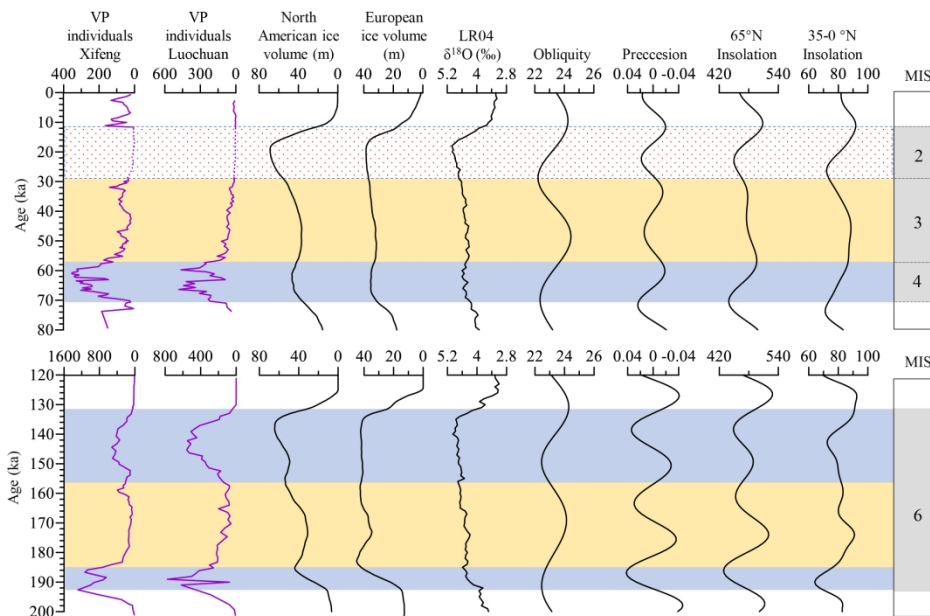
259x295mm (300 x 300 DPI)



338x190mm (300 x 300 DPI)



254x190mm (300 x 300 DPI)



254x190mm (300 x 300 DPI)

Table 1. Selected age-control points for the Xifeng and Luochuan profiles, used to establish a chronology via comparison with a grain-size age model of Hao *et al.* (2012).

Xifeng depth (m)	Luochuan depth (m)	Age (ka)	Unit
0.0	0.0	0.0	S0 top
0.7	0.6	4.6	S0
2.0	1.5	11.7	S0 bottom
3.5	3.0	29.7	L1
4.7	3.7	34.2	L1
4.9	4.2	36.1	L1
5.6	4.8	39.6	L1
6.9	5.8	49.1	L1
8.0	6.8	52.6	L1
8.8	8.0	57.7	L1
9.1	8.1	59.1	L1
12.1	9.9	71.0	L1/S1 boundary
12.4	10.1	73.8	S1
12.6	10.2	85.0	S1
13.3	10.4	96.6	S1
13.5	10.6	101.3	S1
14.0	11.2	112.4	S1
14.9	11.8	130.0	S1/L2 boundary
15.4	11.9	131.9	L2
16.8	13.6	149.4	L2
18.3	14.7	160.4	L2
19.3	15.4	168.9	L2
20.1	16.4	183.3	L2
21.0	17.2	191.0	L2/S2 boundary
21.4	17.4	197.6	S2

Table 2. List of mollusk species identified in loess units L2 and L1 of the Xifeng and Luochuan sections

Family	Genus	Species
Valloniidae	<i>Vallonia</i>	<i>Vallonia tenera</i> (Reinhardt, 1877)
		<i>Vallonia</i> cf. <i>pulchella</i> (Muller, 1774)
Pupillidae	<i>Pupilla</i>	<i>Pupilla aeoli</i> (Hilber, 1883)
		<i>Pupilla</i> cf. <i>muscorum</i> (Linne, 1758)
	<i>Gastrocopta</i>	<i>Gastrocopta armigerella</i> (Reinhardt, 1877)
		<i>Gastrocopta coreana</i> Pilsbry, 1916 <i>Gastrocopta</i> sp.
Endodontidae	<i>Punctum</i>	<i>Punctum orphana</i> (Heude, 1882)
Vertiginidae	<i>Vertigo</i>	<i>Vertigo chenchiaoensis</i> Li, 1966
Succineidae	<i>Succinea</i>	<i>Succinea</i> sp.
Ariophantidae	<i>Macrochlamys</i>	<i>Macrochlamys angigyra</i> Yen, 1939
		<i>Kaliella lamprocystis</i> Moellendorff, 1899 <i>Kaliella</i> sp.
Bradybaenidae	<i>Cathaica</i>	<i>Cathaica pulveratrix</i> (Martens, 1882)
		<i>Cathaica pulveraticula</i> (Martens, 1882)
		<i>Cathaica richthofen</i> (Martens, 1873) <i>Cathaica</i> sp.
	<i>Methodontia</i>	<i>Methodontia yantaiensis</i> (Crosse and Debeaux, 1863)
		<i>Methodontia huaiensis</i> (Crosse, 1882)
		<i>Methodontia beresowskii</i> (Moellendorff, 1899) <i>Methodontia</i> sp.
Subulinidae	<i>Opeas</i>	<i>Opeas striatissimum</i> (Gredler, 1882)
Camaenidae	<i>Trichochloritis</i>	<i>Trichochloritis</i> sp.
Pristilomatidae	<i>Vitrea</i>	<i>Vitrea pygmaea</i> (Boettger, 1880)
Limacidae		

Table S1. Dataset of the number of *Vallonia tenera* and *Pupilla aeoli* (VP) individuals in loess units L2 and L1 from the Xifeng section.

Depth (m)	Age (ka)	Lithology	Magnetic susceptibility	<i>Vallonia tenera</i>	<i>Pupilla aeoli</i>	VP
2	11.7	L1	49.49	2	2	4
2.1	12.9	L1	54.76	4	0	4
2.2	14.1	L1	44.78	4	0	4
2.3	15.3	L1	47.96	1	0	1
2.4	16.5	L1	41.58	0	0	0
2.5	17.7	L1	39.60	0	0	0
2.6	18.9	L1	43.78	3	2	5
2.7	20.1	L1	39.70	3	4	7
2.8	21.3	L1	44.55	6	8	14
2.9	22.5	L1	44.06	5	2	7
3	23.7	L1	43.75	5	3	8
3.1	24.9	L1	46.27	5	5	10
3.2	26.1	L1	46.77	12	5	17
3.3	27.3	L1	49.25	16	10	26
3.4	28.5	L1	53.66	23	15	38
3.5	29.7	L1	54.11	16	18	34
3.6	30.0	L1	63.78	31	29	60
3.7	30.4	L1	53.73	18	24	42
3.8	30.8	L1	57.77	38	28	66
3.9	31.2	L1	64.32	52	36	88
4	31.5	L1	61.03	53	42	95
4.1	31.9	L1	59.33	91	51	142
4.2	32.3	L1	57.51	69	28	97
4.3	32.7	L1	61.27	38	25	63
4.4	33.1	L1	61.00	26	26	52
4.5	33.4	L1	63.05	30	30	60
4.6	33.8	L1	66.17	33	33	66
4.7	34.2	L1	59.33	22	44	66
4.8	35.1	L1	65.20	21	48	69
4.9	36.1	L1	75.13	20	70	90
5	36.6	L1	71.00	20	51	71
5.1	37.1	L1	73.23	13	68	81
5.2	37.6	L1	67.84	26	60	86
5.3	38.1	L1	75.12	27	49	76
5.4	38.6	L1	72.16	33	37	70

1
2
3
4
5
6
7
8
9
10
11
12
13
14
15
16
17
18
19
20
21
22
23
24
25
26
27
28
29
30
31
32
33
34
35
36
37
38
39
40
41
42
43
44
45
46
47
48
49
50
51
52
53
54
55
56
57
58
59
60

5.5	39.1	L1	71.50	26	40	66
5.6	39.6	L1	72.40	16	44	60
5.7	40.4	L1	65.99	8	36	44
5.8	41.1	L1	63.73	9	15	24
5.9	41.8	L1	60.98	9	15	24
6	42.5	L1	67.33	3	16	19
6.1	43.3	L1	66.83	8	19	27
6.2	44.0	L1	67.01	10	11	21
6.3	44.7	L1	65.67	14	20	34
6.4	45.4	L1	64.95	22	21	43
6.5	46.2	L1	66.03	18	20	38
6.6	46.9	L1	72.95	24	74	98
6.7	47.6	L1	69.95	24	53	77
6.8	48.3	L1	71.29	9	68	77
6.9	49.1	L1	58.54	18	31	49
7	49.4	L1	60.10	11	35	46
7.1	49.7	L1	68.53	10	34	44
7.2	50.0	L1	68.23	4	31	35
7.3	50.3	L1	68.81	7	46	53
7.4	50.7	L1	70.71	8	37	45
7.5	51.0	L1	72.92	6	58	64
7.6	51.3	L1	75.86	5	63	68
7.7	51.6	L1	78.28	11	55	66
7.8	51.9	L1	81.41	6	62	68
7.9	52.3	L1	82.90	8	75	83
8	52.6	L1	88.89	11	43	54
8.1	53.2	L1	82.23	8	54	62
8.2	53.9	L1	80.10	19	61	80
8.3	54.5	L1	82.44	30	83	113
8.4	55.2	L1	78.43	18	49	67
8.5	55.8	L1	70.73	30	116	146
8.6	56.5	L1	69.50	35	139	174
8.7	57.1	L1	65.69	21	100	121
8.8	57.7	L1	50.72	51	142	193
8.9	58.2	L1	45.10	53	140	193
9	58.6	L1	42.64	73	130	203
9.1	59.1	L1	36.10	100	162	262
9.2	59.5	L1	39.18	132	194	326
9.3	59.9	L1	36.68	144	176	320
9.4	60.3	L1	38.38	132	187	319
9.5	60.7	L1	42.65	130	222	352
9.6	61.1	L1	36.18	111	243	354

1
2
3
4
5
6
7
8
9
10
11
12
13
14
15
16
17
18
19
20
21
22
23
24
25
26
27
28
29
30
31
32
33
34
35
36
37
38
39
40
41
42
43
44
45
46
47
48
49
50
51
52
53
54
55
56
57
58
59
60

9.7	61.5	L1	38.42	114	198	312
9.8	61.9	L1	37.81	120	221	341
9.9	62.3	L1	36.22	144	191	335
10	62.7	L1	35.61	80	89	169
10.1	63.1	L1	33.16	90	57	147
10.2	63.5	L1	34.83	303	27	330
10.3	63.9	L1	35.68	283	10	293
10.4	64.3	L1	35.68	295	11	306
10.5	64.7	L1	34.69	245	10	255
10.6	65.1	L1	33.33	225	14	239
10.7	65.4	L1	27.27	232	10	242
10.8	65.8	L1	30.46	276	18	294
10.9	66.2	L1	37.24	232	12	244
11	66.6	L1	38.34	268	36	304
11.1	67.0	L1	30.00	206	30	236
11.2	67.4	L1	39.69	172	22	194
11.3	67.8	L1	37.31	108	38	146
11.4	68.2	L1	39.80	112	48	160
11.5	68.6	L1	44.95	137	68	205
11.6	69.0	L1	43.28	115	61	176
11.7	69.4	L1	39.49	59	56	115
11.8	69.8	L1	37.88	33	33	66
11.9	70.2	L1	37.76	14	12	26
12	70.6	L1	37.50	10	12	22
12.1	71.0	L1	58.59	15	34	49
12.2	71.9	S1	97.98	35	20	55
12.3	72.8	S1	117.59	1	4	5
12.4	73.8	S1	120.00	140	45	185
12.5	79.4	S1	98.01	101	50	151
12.6	85.0	S1	116.92	211	50	261
12.7	86.6	S1	100.50	178	81	259
12.8	88.3	S1	114.36	131	68	199
12.9	89.9	S1	105.00	154	138	292
13	91.6	S1	110.45	140	154	294
13.1	93.2	S1	109.50	111	40	151
13.2	94.9	S1	132.16	229	122	351
13.3	96.6	S1	143.28	109	46	155
13.4	98.9	S1	134.00	112	71	183
13.5	101.3	S1	124.75	90	62	152
13.6	103.5	S1	128.36	72	60	132
13.7	105.8	S1	144.28	8	23	31
13.8	108.0	S1	147.26	17	22	39

1
2
3
4
5
6
7
8
9
10
11
12
13
14
15
16
17
18
19
20
21
22
23
24
25
26
27
28
29
30
31
32
33
34
35
36
37
38
39
40
41
42
43
44
45
46
47
48
49
50
51
52
53
54
55
56
57
58
59
60

13.9	110.2	S1	149.49	13	21	34
14	112.4	S1	150.00	6	14	20
14.1	114.4	S1	148.48	58	30	88
14.2	116.3	S1	147.26	7	4	11
14.3	118.3	S1	142.13	1	3	4
14.4	120.2	S1	129.44	3	6	9
14.5	122.2	S1	121.50	1	9	10
14.6	124.1	S1	101.49	16	6	22
14.7	126.1	S1	99.50	7	16	23
14.8	128.0	S1	96.52	9	16	25
14.9	130.0	L2	77.78	13	15	28
15	130.4	L2	65.83	11	19	30
15.1	130.8	L2	61.58	19	37	56
15.2	131.1	L2	41.71	9	30	39
15.3	131.5	L2	34.48	24	32	56
15.4	131.9	L2	31.19	39	23	62
15.5	133.2	L2	48.00	42	40	82
15.6	134.4	L2	32.50	79	99	178
15.7	135.7	L2	30.00	80	104	184
15.8	136.9	L2	32.00	153	106	259
15.9	138.2	L2	32.00	205	178	383
16	139.4	L2	33.00	203	198	401
16.1	140.7	L2	33.17	203	219	422
16.2	141.9	L2	32.66	163	180	343
16.3	143.2	L2	35.35	193	209	402
16.4	144.4	L2	33.83	272	248	520
16.5	145.7	L2	37.44	174	253	427
16.6	146.9	L2	37.37	194	261	455
16.7	148.2	L2	37.50	126	379	505
16.8	149.4	L2	41.00	145	217	362
16.9	150.2	L2	39.49	148	208	356
17	150.9	L2	38.78	76	192	268
17.1	151.6	L2	32.99	78	108	186
17.2	152.3	L2	35.68	46	54	100
17.3	153.1	L2	34.02	69	44	113
17.4	153.8	L2	35.00	62	43	105
17.5	154.5	L2	34.50	152	30	182
17.6	155.3	L2	33.33	182	11	193
17.7	156.0	L2	31.98	193	17	210
17.8	156.7	L2	28.64	209	7	216
17.9	157.4	L2	30.65	254	11	265
18	158.2	L2	31.86	246	4	250

1
2
3
4
5
6
7
8
9
10
11
12
13
14
15
16
17
18
19
20
21
22
23
24
25
26
27
28
29
30
31
32
33
34
35
36
37
38
39
40
41
42
43
44
45
46
47
48
49
50
51
52
53
54
55
56
57
58
59
60

18.1	158.9	L2	32.02	369	27	396
18.2	159.6	L2	31.66	343	12	355
18.3	160.4	L2	39.50	212	11	223
18.4	161.2	L2	32.18	116	14	130
18.5	162.1	L2	29.44	129	26	155
18.6	162.9	L2	29.56	120	13	133
18.7	163.8	L2	31.09	90	38	128
18.8	164.6	L2	32.49	40	26	66
18.9	165.5	L2	37.82	35	39	74
19	166.3	L2	42.86	7	58	65
19.1	167.2	L2	43.88	16	42	58
19.2	168.0	L2	52.45	30	79	109
19.3	168.9	L2	51.02	27	53	80
19.4	170.7	L2	49.74	30	68	98
19.5	172.5	L2	46.50	42	95	137
19.6	174.3	L2	46.00	50	84	134
19.7	176.1	L2	41.00	66	79	145
19.8	177.9	L2	41.00	48	76	124
19.9	179.7	L2	43.00	104	93	197
20	181.5	L2	38.00	134	127	261
20.1	183.3	L2	37.31	129	156	285
20.2	184.1	L2	40.30	256	281	537
20.3	185.0	L2	52.97	415	309	724
20.4	185.9	L2	56.44	553	510	1063
20.5	186.7	L2	61.69	561	568	1129
20.6	187.6	L2	62.69	413	483	896
20.7	188.4	L2	62.50	401	244	645
20.8	189.3	L2	66.00	546	176	722
20.9	190.1	L2	73.63	680	243	923
21	191.0	L2	83.00	759	238	997

Table S2. Dataset of the number of *Vallonia tenera* and *Pupilla aeoli* (VP) individuals in loess units L2 and L1 from the Luochuan section.

Depth (m)	Age (ka)	Lithology	Magnetic susceptibility	<i>Vallonia tenera</i>	<i>Pupilla aeoli</i>	VP
1.5	11.7	L1	41.10	1	0	1
1.6	12.9	L1	41.80	2	1	3
1.7	14.1	L1	34.80	1	0	1
1.8	15.3	L1	37.10	0	3	3
1.9	16.5	L1	30.70	1	2	3
2	17.7	L1	32.80	1	2	3
2.1	18.9	L1	32.40	0	2	2
2.2	20.1	L1	34.10	2	2	4
2.3	21.3	L1	32.50	0	0	0
2.4	22.5	L1	34.00	3	1	4
2.5	23.7	L1	33.40	5	1	6
2.6	24.9	L1	34.50	6	4	10
2.7	26.1	L1	39.10	2	6	8
2.8	27.3	L1	42.70	3	7	10
2.9	28.5	L1	39.70	5	11	16
3	29.7	L1	47.60	5	7	12
3.1	30.3	L1	49.00	12	4	16
3.2	31.0	L1	51.20	8	17	25
3.3	31.6	L1	52.70	17	9	26
3.4	32.2	L1	52.20	25	30	55
3.5	32.9	L1	52.00	23	26	49
3.6	33.5	L1	52.10	27	13	40
3.7	34.2	L1	53.20	18	21	39
3.8	34.6	L1	60.70	1	21	22
3.9	34.9	L1	65.50	6	20	26
4	35.3	L1	66.10	2	16	18
4.1	35.7	L1	65.90	4	30	34
4.2	36.1	L1	70.80	8	27	35
4.3	36.7	L1	70.50	16	3	19
4.4	37.3	L1	69.00	40	6	46
4.5	37.9	L1	70.80	15	15	30
4.6	38.4	L1	66.90	3	36	39
4.7	39.0	L1	67.90	8	51	59
4.8	39.6	L1	68.20	6	71	77
4.9	40.6	L1	73.70	1	47	48

1
2
3
4
5
6
7
8
9
10
11
12
13
14
15
16
17
18
19
20
21
22
23
24
25
26
27
28
29
30
31
32
33
34
35
36
37
38
39
40
41
42
43
44
45
46
47
48
49
50
51
52
53
54
55
56
57
58
59
60

5	41.5	L1	69.90	6	67	73
5.1	42.5	L1	70.90	10	64	74
5.2	43.4	L1	68.40	12	54	66
5.3	44.3	L1	67.60	9	50	59
5.4	45.3	L1	67.70	28	50	78
5.5	46.2	L1	66.50	16	35	51
5.6	47.2	L1	67.20	22	35	57
5.7	48.1	L1	68.80	22	43	65
5.8	49.1	L1	60.00	18	50	68
5.9	49.4	L1	62.70	23	47	70
6	49.8	L1	72.90	29	62	91
6.1	50.1	L1	69.60	43	78	121
6.2	50.5	L1	72.40	42	62	104
6.3	50.8	L1	69.00	30	62	92
6.4	51.2	L1	75.40	10	73	83
6.5	51.5	L1	80.10	4	90	94
6.6	51.9	L1	75.70	12	86	98
6.7	52.2	L1	83.10	4	75	79
6.8	52.6	L1	88.10	7	67	74
6.9	53.0	L1	81.30	2	62	64
7	53.4	L1	78.70	2	74	76
7.1	53.9	L1	69.90	0	81	81
7.2	54.3	L1	64.10	0	98	98
7.3	54.7	L1	65.60	7	119	126
7.4	55.2	L1	65.50	27	132	159
7.5	55.6	L1	66.20	10	79	89
7.6	56.0	L1	62.80	9	101	110
7.7	56.5	L1	53.80	34	93	127
7.8	56.9	L1	55.40	38	147	185
7.9	57.3	L1	55.80	59	205	264
8	57.7	L1	49.10	63	189	252
8.1	59.1	L1	33.30	92	214	306
8.2	59.8	L1	33.80	195	270	465
8.3	60.4	L1	33.90	95	156	251
8.4	61.1	L1	34.80	77	104	181
8.5	61.7	L1	31.60	109	110	219
8.6	62.4	L1	31.40	72	55	127
8.7	63.1	L1	34.60	43	46	89
8.8	63.7	L1	37.20	225	195	420
8.9	64.4	L1	34.40	181	166	347
9	65.1	L1	36.00	216	227	443
9.1	65.7	L1	37.80	114	226	340

1							
2							
3							
4	9.2	66.4	L1	38.40	242	241	483
5	9.3	67.0	L1	37.30	142	105	247
6	9.4	67.7	L1	37.50	155	154	309
7	9.5	68.4	L1	43.50	88	122	210
8	9.6	69.0	L1	41.40	89	126	215
9	9.7	69.7	L1	48.20	117	117	234
10	9.8	70.3	L1	50.80	110	107	217
11	9.9	71.0	L1	71.30	64	17	81
12	10	72.4	S1	73.70	41	32	73
13	10.1	73.8	S1	129.30	22	16	38
14	10.2	85.0	S1	104.50	12	11	23
15	10.3	90.8	S1	111.40	6	20	26
16	10.4	96.6	S1	128.30	9	33	42
17	10.5	98.9	S1	114.40	22	23	45
18	10.6	101.3	S1	105.80	25	31	56
19	10.7	103.2	S1	131.60	41	17	58
20	10.8	105.0	S1	132.80	63	32	95
21	10.9	106.9	S1	161.40	28	12	40
22	11	108.7	S1	170.80	18	11	29
23	11.1	110.6	S1	168.00	5	4	9
24	11.2	112.4	S1	180.30	0	0	0
25	11.3	115.4	S1	171.20	4	0	4
26	11.4	118.3	S1	165.60	3	1	4
27	11.5	121.2	S1	154.20	0	0	0
28	11.6	124.1	S1	122.70	0	0	0
29	11.7	127.1	S1	97.50	0	0	0
30	11.8	130.0	L2	74.90	0	0	0
31	11.9	131.9	L2	23.30	18	34	52
32	12	132.9	L2	25.20	31	44	75
33	12.1	134.0	L2	24.40	60	121	181
34	12.2	135.0	L2	21.50	68	122	190
35	12.3	136.0	L2	24.40	107	190	297
36	12.4	137.1	L2	24.70	197	213	410
37	12.5	138.1	L2	25.10	169	293	462
38	12.6	139.1	L2	27.10	226	284	510
39	12.7	140.2	L2	29.20	227	253	480
40	12.8	141.2	L2	31.80	194	249	443
41	12.9	142.2	L2	32.10	217	333	550
42	13	143.3	L2	33.00	197	314	511
43	13.1	144.3	L2	33.80	185	352	537
44	13.2	145.3	L2	33.80	269	288	557
45	13.3	146.3	L2	36.10	213	316	529
46							
47							
48							
49							
50							
51							
52							
53							
54							
55							
56							
57							
58							
59							
60							

1
2
3
4
5
6
7
8
9
10
11
12
13
14
15
16
17
18
19
20
21
22
23
24
25
26
27
28
29
30
31
32
33
34
35
36
37
38
39
40
41
42
43
44
45
46
47
48
49
50
51
52
53
54
55
56
57
58
59
60

13.4	147.4	L2	34.70	136	244	380
13.5	148.4	L2	34.70	183	208	391
13.6	149.4	L2	36.10	176	172	348
13.7	150.4	L2	33.70	173	161	334
13.8	151.4	L2	30.00	210	96	306
13.9	152.4	L2	30.20	131	43	174
14	153.4	L2	30.70	145	64	209
14.1	154.4	L2	27.50	153	40	193
14.2	155.4	L2	25.60	84	84	168
14.3	156.4	L2	27.00	77	62	139
14.4	157.4	L2	24.00	55	21	76
14.5	158.4	L2	23.10	54	25	79
14.6	159.4	L2	24.50	78	23	101
14.7	160.4	L2	30.30	98	25	123
14.8	161.6	L2	30.20	88	24	112
14.9	162.8	L2	32.50	65	18	83
15	164.0	L2	41.40	48	29	77
15.1	165.2	L2	53.60	29	170	199
15.2	166.4	L2	60.50	44	53	97
15.3	167.7	L2	71.60	31	38	69
15.4	168.9	L2	72.80	29	64	93
15.5	170.3	L2	59.10	16	43	59
15.6	171.8	L2	68.20	25	103	128
15.7	173.2	L2	68.90	36	138	174
15.8	174.6	L2	64.70	31	70	101
15.9	176.1	L2	51.50	65	93	158
16	177.5	L2	43.30	125	88	213
16.1	179.0	L2	39.10	154	57	211
16.2	180.4	L2	35.60	130	93	223
16.3	181.8	L2	35.20	122	84	206
16.4	183.3	L2	33.70	113	99	212
16.5	184.2	L2	38.20	153	148	301
16.6	185.2	L2	43.40	116	139	255
16.7	186.2	L2	46.20	202	218	420
16.8	187.1	L2	52.80	268	188	456
16.9	188.1	L2	56.00	273	229	502
17	189.1	L2	61.40	469	308	777
17.1	190.0	L2	74.80	55	19	74
17.2	191.0	L2	82.50	415	204	619